Parametric amplification and squeezing of a mode-locked pulse train: A comparison of $MgO:LiNbO_3$ with bulk periodically poled $LiNbO_3$

E. M. Daly and A. I. Ferguson
Department of Physics and Applied Physics, University of Strathclyde, 107 Rottenrow, Glasgow G4 0NG, United Kingdom
(Received 4 August 1999; revised manuscript received 9 March 2000; published 13 September 2000)

We report on an initial squeezing of 3.3 dB below the shot noise level, generated in bulk, quasi-phase-matched lithium niobate. This squeezing was generated by degenerate parametric amplification, at 1047 nm, of a mode-locked pulse train. We present a detailed comparison of the process performed in both the quasi-phase-matched material and in $MgO:LiNbO_3$, which was phase matched using conventional birefringent methods. The single-pass gain measured was 2.5 from $MgO:LiNbO_3$ and 3.9 from periodically poled lithium niobate (PPLN), although the former was affected by photorefractive damage. We directly recorded 11% of noise reduction in the vacuum using the PPLN parametric amplifier, purely because the detection efficiency was so low in our experiment. The experimental data was fitted to a model which includes the initial squeezing level and the homodyne detector efficiency as free parameters. The observed squeezing agrees well with the a total detection efficiency of just 16% and an initial squeezing level of 3.3 dB (53%) in PPLN.

PACS number(s): 42.50.Dv, 42.65.Ky

I. INTRODUCTION

The topic of quasi-phase-matching (QPM) and quantum noise reduction in parametric amplification was first considered theoretically by Bencheikh *et al.* [1] in 1995. It was not immediately clear that QPM in $\chi^{(2)}$ media could give rise to squeezed states of the electromagnetic field, because unlike birefringent phase matching, where the pump and signal fields remain in phase throughout the material, the technique of QPM rephases the waves periodically. The polarity of the medium is inverted, with a period equal to half the coherence length for first-order phase matching, to compensate for the phase difference which builds up between the pump and signal fields [2]. This first theoretical study showed that a quasi-phase-matched parametric amplifier could provide noiseless amplification in one quadrature, and squeezing in the conjugate quadrature of a corresponding amount. One of the differences between this case and parametric amplification in a homogeneous material is that the relative phases between the pump and signal beam for which amplification and deamplification occur are shifted by $\pi/2$; the extra phase shift is introduced entirely in the first half-period of the QPM device. Another difference is that the magnitude of the gain provided by the QPM amplifier is less than that which would result in a perfectly phase-matched homogeneous material. However, this is not a serious flaw because QPM allows one to utilize the large diagonal nonlinear coefficients that birefringent phase matching cannot always access. Furthermore, use of QPM waveguide devices provides careful spatial mode control which leads to a more efficient interaction between the driving pump field and the signal seed. Chickarmane and Agarwal [3] also predicted that the greatest amount of squeezing is generated for the lowest order of phase matching in a QPM amplifier.

In recent years, one of the most widely used and successful QPM materials has been periodically poled lithium niobate, known as PPLN (see for example, Refs. [4–8]). Its attractiveness lies in its large nonlinearity, and the ability to phase match any optical interaction within the transparency range of lithium niobate (0.35–5 μm). To the best of our knowledge there have been just two reports of parametric amplification to produce quantum effects in QPM $LiNbO_3$—one in a waveguide and one in a bulk crystal. Squeezing of the vacuum using single-pass parametric amplification in a QPM $LiNbO_3$ waveguide was reported by Serkland *et al.* [9]. At 1064 nm, the degenerate gain provided by 20-ps mode-locked pulses was 1.9, and the observed squeezing was 14% below the shot noise level. The rationale for using a waveguide to perform the squeezing is to avoid gain-induced diffraction (spatial distortion of the signal beam at high gains), which often plagues similar experiments performed in a single pass through bulk crystals. On the other hand, the longer interaction lengths in waveguides mean that processes which are parasitic on squeezing, such as two-photon absorption or blue-light-induced red absorption [10], can be enhanced. The solution is to reduce the pump power or use longer pump pulses, but these imply less parametric gain and therefore squeezing. In Ref. [9], heating in the waveguide meant that it was necessary to reduce the pump power with an acousto-optic modulator which chopped the mode-locked pulse train at a rate of 400 Hz. Noiseless amplification was also demonstrated in bulk PPLN [11]; the maximum gain provided by the 35-ps-long *Q*-switched pump pulses was 2.5 for a weak signal input at 1054 nm. Until the work described in this paper, there has been no experimental demonstration of quadrature-phase squeezing in bulk periodically poled lithium niobate.

In this work we compare the performance of two bulk crystals—magnesium-oxide-doped lithium niobate ($MgO:LiNbO_3$) and periodically poled lithium niobate (PPLN)—for single-pass parametric amplification at 1047 nm pumped by cw mode-locked pulses. The compact all-solid-state system we describe provided 3-ps-long pulses at a repetition rate of 140 MHz, resulting in extremely high peak powers for modest average powers. We found that the $MgO:LiNbO_3$ crystal was very strongly affected by the high

pump intensities used. In order to measure the parametric gain of 2.5, it was necessary to chop the pump beam to reduce its average power. This photorefractive damage prevented any squeezing measurements in MgO:$LiNbO_3$, but was completely absent in PPLN. The bulk PPLN sample amplified a weak signal beam at 1047 nm by a factor of 3.9, and deamplified it by a factor of 0.46 with no signs of any damage to the crystal. With this sample, 0.5 dB of squeezing in the vacuum was observed directly using balanced homodyne detection, despite very large losses (84%) in the detection process. Over 3 dB of squeezing is inferred given the average deamplification factor of 0.46, and assuming perfect detection efficiency. However, at the temporal peak of the pulses, and in the center of the focused region, there is the potential for much more squeezing below the shot noise level.

II. NONLINEAR MATERIALS

Phase-sensitive parametric amplification at 1047 nm was studied in the two samples. Type-I noncritical phase matching (NCPM) was employed in both cases, thus ensuring no spatial walk-off between the pump and signal beams as they propagated together through the crystals. The crystals were mounted in ovens so that they could be heated to their respective NCPM temperatures.

Conventional birefringent phase matching was employed to perform phase-sensitive amplification of the signal field in the first material, MgO:$LiNbO_3$. To satisfy the phase-matching conditions for this interaction, the pump was polarized as an extraordinary wave, the signal was polarized as an ordinary wave, and propagation was along the y axis; xyz here refer to the principal axes of the refractive index ellipsoid. Pure $LiNbO_3$ has a low optical damage threshold which is a result of photorefractive damage [12]. The susceptibility to this type of damage can be lessened by doping with MgO, which produces a shift in the absorption edge of the material toward the blue [13]. The MgO:$LiNbO_3$ sample used in this study was antireflection coated at both the signal and pump wavelengths in an attempt to minimize losses in the squeezing experiment.

To access the largest component of the susceptibility tensor d_{333} in the PPLN experiment, both pump and signal beams were polarized as extraordinary waves. This test sample was 0.5 mm thick and 5 mm long in the direction of light propagation. It contained six gratings (regions where the sign of $\chi^{(2)}$ is modulated): two each of 6.24, 6.36, and 6.57 μm. These were designed for second-harmonic generations of 1047, 1053, and 1064 nm, respectively, at a phase-matching temperature of about 160 °C, and were arranged symmetrically in the center of the sample. This crystal was not antireflection coated at any wavelength, and the measured transmission was only about 76% at 1047 nm, which is consistent with a Fresnel loss of 13% at both the entrance and exit faces of the sample [14]. The transmission of the pump was not measured, but we estimate that 15% of the incident pump power was reflected from the uncoated front face at this wavelength. PPLN has been shown to be less prone to photorefractive damage than the unpoled material—possibly because of a cancellation effect in the alternating domains [4,15]. In addition, operation of the crystal at elevated temperatures helps to disperse the carriers which cause the effect.

TABLE I. Some physical properties of the two nonlinear crystals used in this study of optical parametric amplification. The effective nonlinear coefficients for both crystals, and the Sellmeier coefficients for MgO:$LiNbO_3$, were taken from the ''Caladox Limited'' crystal components catalog.

Crystal	MgO:$LiNbO_3$		PPLN
Length (mm)	3		5
Phase-matching temperature (°C)	70		160
d_{eff}(pm/V)	$d_{311}=4.7$		$\frac{2}{\pi}d_{333}=17.6$
Principle indices [35]	n_o	n_e	n_e
$\lambda=1047$ nm	2.225	2.147	2.163
$\lambda=523.5$ nm	2.319	2.225	2.246
Group velocity walk-off (ps/mm)	0.69		1.03
$\Delta\nu$ (GHz)	120		150
Theoretical γ_{shg} (W^{-1})	4.2×10^{-4}		8×10^{-3}
Experimental γ_{shg} (W^{-1})	3.1×10^{-4}		6.4×10^{-4}

A. Sample characterization

Some relevant physical properties of the two samples used are listed in Table I. The strength of the nonlinearity (and therefore the potential for large amounts of squeezing) in each material was first estimated by measuring the single-pass conversion factor γ_{shg} for second-harmonic generation of the Nd:YLF laser output in each crystal. The conversion factor, for the cw case, can also be calculated from [16]

$$\gamma_{shg}(cw)=\left(\frac{16\pi^2 d_{eff}^2 l}{n_{2\omega}n_{\omega}\lambda^3\epsilon_o c}\right)h(B,\xi), \tag{1}$$

where l is the crystal length, λ is the fundamental wavelength, and n_ω and $n_{2\omega}$ are the refractive indices of the fundamental and second-harmonic waves. The exact value of the Boyd-Kleinman focusing factor $h(B,\xi)$ depends upon the double-refraction parameter B and the focusing conditions determined by the focusing parameter ξ [17]. This is given by

$$\xi=\frac{l}{b}=\frac{\lambda}{2\pi n_\omega}\frac{1}{\omega_o^2}, \tag{2}$$

where b is the confocal parameter, and ω_o is the spot size of the focused beam. The analysis of parametric interactions using focused Gaussian beams, performed by Boyd and Kleimman, showed that the greatest efficiency is obtained when there is no spatial walk-off, and when the focusing conditions are arranged so that $\xi=2.84$. The NCPM employed in this work implies no walk-off between the pump and signal fields, so $B=0$ in Eq. (1), and all that remains is to adjust the spot size in the crystal carefully. The expression for the conversion efficiency is modified slightly when short

pulses, with correspondingly large frequency bandwidths, are considered. $\gamma_{shg}(cw)$ is multiplied by a factor

$$F_\nu = \sqrt{\frac{\Delta\nu^2}{\Delta\nu_L^2 + \Delta,\nu^2}}, \tag{3}$$

where $\Delta\nu$ is the spectral acceptance bandwidth of the nonlinear crystal, and $\Delta\nu_L$ is the bandwidth of the laser pulse [18]. The doubling efficiency for pulsed operation is therefore given by

$$\gamma_{shg} = \gamma_{shg}(cw)F_\nu, \tag{4}$$

and, in order to maximize this quantity, it is desirable to use a crystal which has a spectral acceptance bandwidth which is much larger than the bandwidth of the pulse to be doubled. In our experiment, while $\Delta\nu$ was greater than $\Delta\nu_L$ for both crystals used, the magnitudes were comparable, and so F_ν was significantly less than unity. Using the measured bandwidth of the laser, which was found to be 110 GHz, and the calculated values of $\Delta\nu$ listed in Table I, we find that $F_\nu = 0.54$ for the MgO:$LiNbO_3$ crystal and 0.81 for the PPLN crystal. Assuming the optimum focusing arrangement gives theoretical values for γ_{shg} of 4.2×10^{-4} W^{-1} for MgO:$LiNbO_3$ and 8×10^{-3} W^{-1} for PPLN.

γ_{shg} was actually measured by focusing a small fraction of the Nd:YLF output into the crystals using mode-matching conditions designed to produce the optimum spot sizes. The fundamental light was filtered out, and the second-harmonic intensity was recorded with a large-area silicon photodiode of known response at this wavelength. The discrepancy between the theoretical and experimental values listed in Table I can probably easily be explained by a small deviation of the focused spot size in MgO:$LiNbO_3$ from that required to set $\xi = 2.84$, resulting in a reduction of $h(0,\xi)$ below its ideal value of unity. The much larger divergence between theory and experiment for PPLN may be caused by several factors. It may be the case that the available d_{eff}, in this particular test sample, is smaller than the theoretical magnitude listed in Table I. Indeed, examination of the grating quality after poling did indicate some imperfections. The low experimental second-harmonic efficiency may also be due to the relatively large group-velocity walk-off between the fundamental and second-harmonic pulses in the 5-mm-long sample. The group velocity walk-off gives the temporal separation of the center of the signal and pump pulses after propagation through a given length of material. This is an important factor to consider when dealing with short pulses of the order of picoseconds, and in this work, where the signal pulse duration was just 3 ps, it restricted us to the use of relatively short samples. Ideally, one would like to arrange for the fundamental and second-harmonic pulses to be perfectly overlaped over the entire interaction length. For example, if the length of the PPLN sample were reduced to just 3 mm, then the temporal walk-off of the pulse peaks would have been just 3 ps over the crystal length, instead of 5 ps, and the spectral acceptance bandwith would have been increased to 250 GHz, giving $F_\nu = 0.9$. The performance of a parametric amplifier, which is dependent upon the interaction between a weak signal and a strong pump pulse, will also be affected by any temporal walk-off between these two fields. From the measured values of γ_{shg}, we expect that PPLN should provide the largest parametric gain—but that this would still be less than ideal for this particular material.

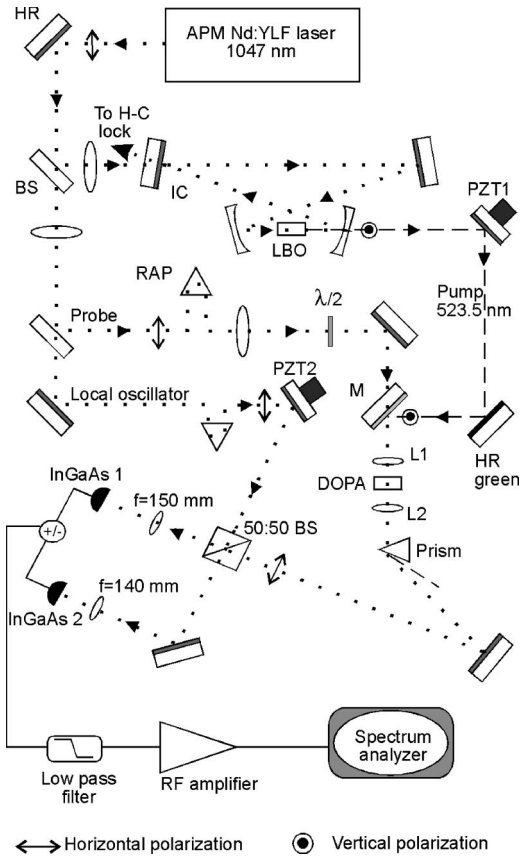

FIG. 1. Schematic diagram of the experimental setup for degenerate parametric amplification and squeezing using picosecond pulses. Dotted line, 1047 nm; dashed line, 523.5 nm; BS, beam splitter; IC, input coupler; HR, high reflector; CHR, curved high reflector at 1047 nm and high transmitter at 523.5 nm; M, mirror to combine pump and probe; DOPA, degenerate optical parametric amplification; PZT1, relative phase between the pump and probe; PZT2, relative phase between LO and squeezed vacuum; and RAP, right angled prism for delay lines.

III. EXPERIMENTAL DETAILS

A schematic diagram of the experimental setup used for parametric amplification and squeezing is shown in Fig. 1. The pump source for optical parametric amplification was a green beam at 523.5 nm, with an average power of 0.45 W. This was generated by frequency doubling the mode-locked pulse train from the Nd:YLF laser (horizontal polarization) in an external enhancement cavity using the nonlinear material lithium niobate. The pump light (vertical polarization) exited from the enhancement cavity through a dichroic mirror, which was highly reflecting for the laser light, but had 92% transmission for the doubled light. A small amount ($\sim$1 mW) of the laser light was split off to form a weak probe and local oscillator (LO) beam; the probe was used to

TABLE II. Required beam waists w_o for maximum parametric gain using NCPM.

	$MgO:LiNbO_3$		PPLN	
Confocal parameter (mm)	1.1		1.8	
w_o (μm)	pump	signal	pump	signal
	6.4	9.1	8.1	11.5

align the amplifier and balanced homodyne detector (BHD) and to investigate the classical response of the amplifier, while the LO propagated to the BHD for pulsed squeezing measurements [19–21]. The probe and pump beams were then combined in the nonlinear crystal which was being used to perform the amplification. Assuming Gaussian beam profiles, the beam parameters of the pump and probe were carefully modeled, so that the beam-shaping optics in each path could be arranged to maximize the parametric gain. It transpires that for NCPM, because there is no spatial walk-off, the optimum beam waists for the signal and pump in parametric amplification can be evaluated from the exact same formula as that used to determine the fundamental beam waist in frequency doubling [17]. The optimum spot sizes w_o, at both the probe and pump wavelengths, were calculated for each crystal using Eq. (2), and the desired values are listed in Table II. The experimental beam waists were then measured by recording the percentage of light which was transmitted through a precision pinhole of 5- or 10-μm diameter. The positions of the lenses in each path were then fine-tuned to attain the required radii at the waists. The pinhole was also used to ensure that the pump and probe beams overlapped spatially. As the position of the pump and probe waists, after the final lens in each path, was extremely critical for the short crystals, aspheric lenses ($f=18.4$ mm Thorlabs C280TM-B) were used to complete the mode matching into the parametric amplifier. In Fig. 1, $L1$ and $L2$ are short-focal length lenses for focusing into and out of the parametric amplifier crystals; $L1$ was antireflection coated at the pump wavelength, and $L2$ at the wavelength of squeezing—1047 nm.

Because the experiment was performed with a source which consisted of a train of mode-locked pulses, it was necessary for the pump and probe pulses to overlap temporally in the nonlinear crystal if any interaction was to take place. The relative arrival time of the pulses was varied by having the probe beam pass through a delay line, consisting of a right-angled prism mounted on a translation stage. This prism did not alter the duration of the laser pulses, as autocorrelation measurements taken with and without the prism in place were identical. In addition, one of the mirrors in the probe beam path was placed on a piezoelectric transducer to enable the relative phase between the two beams to be scanned. At the output of the amplifier, a prism was used to separate the strong pump from the amplified probe, so that its intensity could be monitored with a large-area silicon photodiode. This prism was used at Brewster's angle for the probe light in order to minimize reflection losses at 1047 nm.

At the balanced homodyne detector, the squeezed signal was interfered with the LO beam at a 50:50 beam splitter, and the output from both ports was recorded using high-efficiency $Ga_xIn_{(1-x)}As$ *p-i-n* photodiodes with an active area of 300 μm diameter (Epitaxx ETX 300T). The combined output from both photodiodes was arranged to be their difference photocurrent. This was fed through a low-pass filter (dc to 20 MHz) to reduce the signal at the laser repetition rate, and through a rf amplifier (Trontech W110B-13) which provided a power gain of 50–52 dB for frequencies out to 110 MHz. The amplifier output was, in turn, passed to a rf spectrum analyser (Tektronix 2710) which measured the noise power. The output from the spectrum analyzer (-1.6 V$\equiv 8$ dBm) was displayed on a digital oscilloscope that was read by a personal computer to provide data collection. During squeezing measurements the LO power was maintained well below that required to saturate the photodiodes—approximately 3 mW for a tightly focused beam. The detector photocurrents were typically balanced to 20–30 dB at rf frequencies of several MHz, with the best balance occurring at about 2 MHz. As the relative phase between the squeezed and LO beams is scanned, the LO samples the noise in the quadratures of the squeezed light.

IV. EXPERIMENTAL PARAMETRIC GAIN

A. $MgO:LiNbO_3$

As the relative phase between the pump and probe beams was scanned, the probe exhibited a phase-dependent variation in intensity above and below the dc level measured when the pump was off. The $MgO:LiNbO_3$ sample amplified the probe beam by a factor of 2.5, and deamplified it by a factor of 0.4. However, as has been pointed out, it was necessary to focus the pump beam to a waist with a radius of approximately 6 μm so that parametric gain could be optimized in this very short crystal. These conditions resulted in extremely high green peak powers which caused thermal damage, and quickly reduced the amount of gain observed. With $MgO:LiNbO_3$, the observed gain was reduced by as much as 50% after about a 1-s exposure to the strong pump. Moving the focused beams onto a new position within the crystal would immediately result in an increase in gain, which would then decrease slowly as the high pump power remained incident at that position. After the experiment, when the $MgO:LiNbO_3$ sample had cooled down, it showed signs of permanent damage. In an attempt to overcome this thermal damage problem, the pump beam was chopped to reduce its average power significantly while maintaining high peak power; a duty cycle of 1:20 was typical. Under these conditions, the maximum amplification and deamplification values were recorded, but it is highly likely that the gain we measured was not optimized. Figure 2 shows the measured maximum amplification and deamplification values versus peak pump power for $MgO:LiNbO_3$. It includes the experimental values of 1/deamplification, as this is a useful way to check for any gain-induced diffraction effects. If the two sets of data points (amplification and inverse deamplification factors) are well overlapped, this is normally a sign that no modifications to the signal beam are taking

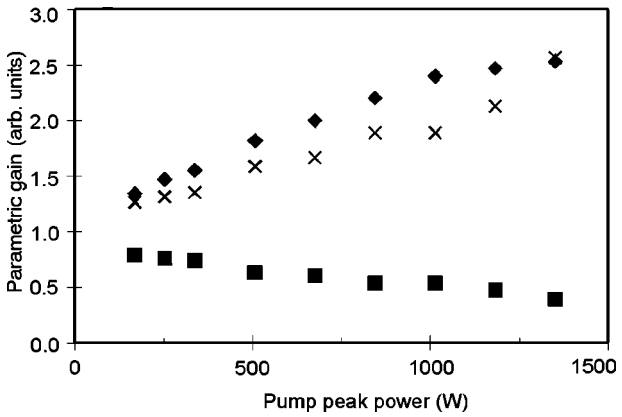

FIG. 2. Gain vs peak pump power for MgO:$LiNbO_3$. The filled data points give deamplification (squares) and amplification (diamonds), while the crosses mark the inverse of the deamplification factors.

place. If they differ appreciably it may mean that the signal spatial and temporal profile is being changed by the focused and pulsed pump beam [22].

B. Bulk PPLN

Of the two gratings on the PPLN sample designed for second-harmonic generation of 1047 nm, it was found that one performed significantly better than the other, so this one was used for all gain measurements (and the second-harmonic efficiency measurements already discussed). Both the 523.5-nm pump beam and the 1047-nm probe needed to have vertical polarization in order to access d_{333}. The pump beam was already vertically polarized on exiting from the enhancement cavity; the probe polarization was controlled with a $\lambda/2$ wave plate before it entered the PPLN crystal. A second $\lambda/2$ wave plate was placed in the probe beam after it exited from the amplifier. This rotated the probe polarization back to horizontal, to reduce reflection losses at the prism which was used to separate it from the pump. At the phase-matching temperature, and with maximum pump power incident on the crystal, the probe beam was amplified by a factor of 3.9 and deamplified by a factor of 0.46, although the best deamplification factor measured was 0.38. Figure 3 shows how the probe intensity at the amplifier output varied as the relative phase between the pump and probe was scanned. The interesting result here is that the PPLN sample did not seem to suffer any thermal damage at all due to the high peak powers of the pump, in stark contrast to the behavior of MgO:$LiNbO_3$. With PPLN, there was no need to reduce the average power of the pump, and no change in the gain was observed as the pump remained incident at one position on the sample. This behavior confirms the resistance of PPLN, used at high temperatures, to photorefractive damage. Figure 4 shows the maximum amplification and deamplification measured in the sample as a function of pump power. It also includes the data set which corresponds to the inverse of deamplification.

In both samples studied, the data series corresponding to the inverse of deamplification as a function of peak pump power did not overlap the amplification points, with the discrepancy being much larger for PPLN than for MgO:$LiNbO_3$. This type of behavior was noted before; for pumping with *Q*-switched pulses, Rarity *et al.* [23] and Kim *et al.* [24] noted the same effect with KTP amplifiers, and Lovering *et al.* [11] in bulk PPLN. Although plane-wave theory predicts a symmetry between amplification and deamplification, it cannot account for the use of focused Gaussian beams and/or short pulses which impart a spatial and temporal dependence to the gain. Parametric gain is usually recorded using direct detection, a technique which averages the measurement temporally over the signal pulse profile, and spatially over the area of the detector which is illuminated. La Porta and Slusher [22] discussed the spatial problem for single-pass parametric amplification in detail, and pointed out that, as the parametric gain is increased, the difference between the predictions of plane-wave theory and the gain measured in direct detection becomes much more noticeable. Our results are consistent with this point, because the disparity in this work is largest in the PPLN sample which provides the largest gain. Identical measurements, using the same ex-

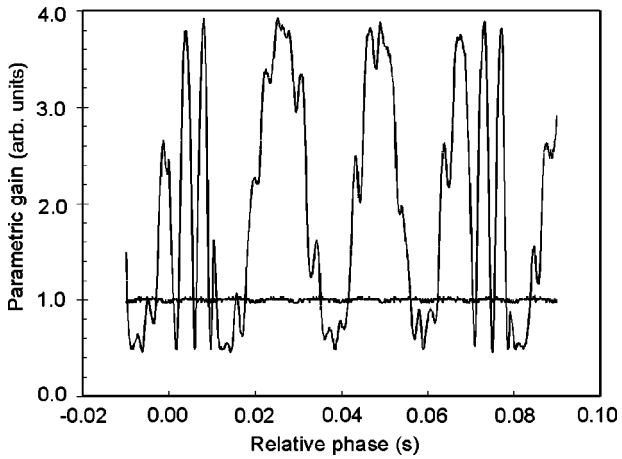

FIG. 3. Parametric amplification and deamplification in PPLN as the relative phase between the pump and probe beams is varied slowly.

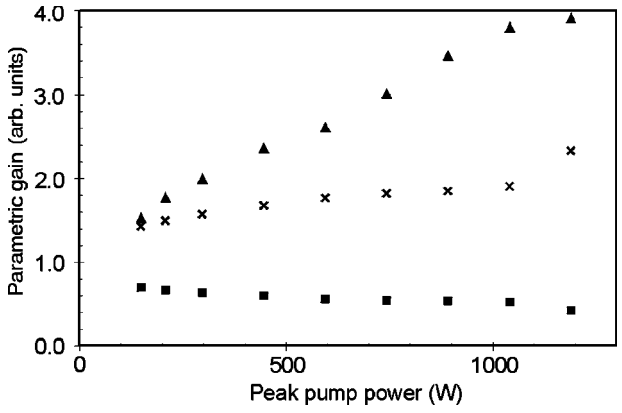

FIG. 4. Parametric amplification and deamplification in PPLN as a function of peak pump power. The pump peak power has been adjusted to take into account the Fresnel loss at this wavelength at the uncoated front surface of the sample. Diamonds, amplification; squares, deamplification; and crosses, inverse of deamplification.

perimental setup, of parametric gain in lithium triborate—a material with a much smaller non-linear coefficient—showed hardly any difference between the amplification and deamplification responses [25]. These points, and the issue of the spatial and temporal dependences of the single-pass parametric gain, will be considered in detail in a separate publication. Here we merely state that a high-quality bulk PPLN sample, of the correct length to minimize group-velocity walk-off, has the potential to provide very high parametric gains, and therefore squeezing, at the spatial and temporal peaks of the pump field. Detection of this squeezing would be complicated, requiring a spatial filtering of the optical parametric amplification output and some type of temporal selection to gather light close to the propagation axis and around the temporal peak of the pulse.

C. Spontaneous parametric fluorescence

Even in the absence of any input, apart from the driving pump field, the parametric amplifier spontaneously emits photons at the signal wavelength—spontaneous parametric fluorescence (SPF) [26]. A reverse-biased $Ga_{1-x}In_xAs$ photodiode was used to measure the total power of SPF, at 1047 nm, generated in PPLN. Because the amount of fluorescence was expected to be quite small, the pump beam was chopped, and the signal at the chopping frequency was recorded using a lock-in amplifier (SRS SR830); the total power was then calculated from the known response of the $In_xGa_{1-x}As$ photodiode. Once all transmission losses had been taken into account, the total average power of SPF generated in PPLN was estimated to be 2.4 nW, or 90 photons/pulse at the laser wavelength. It was possible to check that the SPF had the correct polarization (vertical) expected from the phase-matching conditions, and that the power generated was not enhanced by focusing [27]. Unfortunately it was not possible, with this particular detection scheme, to investigate the change in power as the solid angle subtended by the detector was varied, or to measure the spectrum of fluorescence, because of the low signal power. Measurement of this spectrum would allow one to determine the bandwidth over which squeezing takes place.

V. SQUEEZED VACUUM IN PPLN

When the signal input to the degenerate parametric amplifier is the vacuum state, rather than a probe beam at 1047 nm, the process of parametric amplification produces spontaneous parametric fluorescence at this wavelength. Because of its extremely weak amplitude, and its nonclassical noise properties, this fluorescence is called a squeezed vacuum. The noise properties of the squeezed vacuum, generated in PPLN, were investigated by interfering it with the LO at the laser frequency. In the experiment the average LO power was just 2.5 mW, resulting in a photocurrent in each $In_xGa_{1-x}As$ detector of just under 1 mA; this was well below the level where saturation of the photodiodes may start to occur. A precision pinhole was used to ensure that the LO and squeezed beams filled a large portion of the surface area of the detectors, so as to avoid local saturation effects. The LO radii were estimated to be 75 μm at $In_xGa_{1-x}As$ 1 and 65 μm at $In_xGa_{1-x}As$ 2. The squeezed vacuum radii could only be inferred by a measurement of the probe alignment beam radii; these were estimated to be 80 μm at $In_xGa_{1-x}As$ 1 and 75 μm at $In_xGa_{1-x}As$ 2.

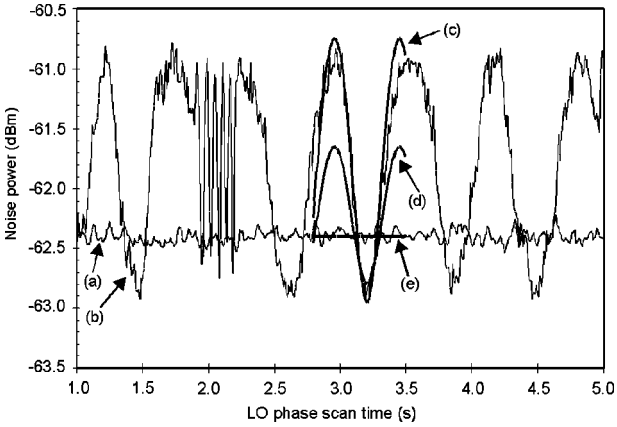

FIG. 5. Detection of the squeezed vacuum in PPLN at a fixed frequency of 2 MHz as the LO phase is scanned slowly. The resolution bandwidth was 300 kHz, and the video filter averaging bandwidth was 30 Hz. The flat line at -62.4 dBm is the SNL (a), while the squeezed vacuum exhibits a phase-dependent noise power (b). Trace (c) is obtained from Eq. (9), with $\eta=0.16$ and $r=0.68$. Trace (d) has $r=0.39$, and trace (e) has $r=0$.

Before performing any squeezing measurements, it was important to check that the laser amplitude fluctuations truly reflected the shot-noise level (SNL). This level was obtained by blocking the output from the degenerate optical parametric amplifier to the homodyne detector and, for the LO power used, the SNL lay 9 dB above the electronic amplifier noise. When the LO was directed to the homodyne detector, but the other input to the 50:50 beam splitter was blocked, the noise power of the sum and difference photocurrents from the $In_xGa_{1-x}As$ detectors agreed to within 0.1 dB at frequencies greater than a few hundred kHz. This shows that the LO beam was shot noise limited at the frequency of interest. More rigorous checks of the laser fluctuations were also carried out by measuring the rf noise power which resulted when a dc photocurrent of known magnitude was generated at one of the detectors. When the SNL is confirmed, then one can be confident that the noise power measured in subsequent squeezing experiments is due solely to vacuum fluctuations.

When the squeezed vacuum was directed to the BHD, the noise power of the difference photocurrent varied in a phase-sensitive way. A trace showing squeezed vacuum at 1047 nm, generated by degenerate parametric amplification in PPLN, is shown in Fig. 5. The rf detection frequency was 2 MHz, and the electronic background noise was subtracted from all data. The noise maxima and minima are about 1.6 dB above and 0.5 dB below the SNL.

A. Effect of losses on squeezed vacuum

The losses which degraded observable squeezing in PPLN were estimated by multiplication of the individual components as described in Ref. [25]. Imperfect quantum efficiency

of the $In_xGa_{1-x}As$ photodiodes contributed a factor of $\eta_d = 0.865$. This was determined experimentally by recording the photocurrent, which resulted when the incident power on each $In_xGa_{1-x}As$ detector was varied. The temporal mismatch between the LO and squeezed vacuum pulse durations added $\eta_t = 0.5$ [28], and $\eta_s = 0.8$ accounted for a spatial overlap of the squeezed and LO beams. This last factor was estimated by measuring the contrast in the interference fringes obtained when the LO and probe fields were mixed at the 50:50 beam splitter. The overlap of the two beams was extremely sensitive to the exact position of the short focal length ($f = 18$ mm) lens in the squeezed beam path directly after the DOPA—$L2$ in Fig. 1, so this value of η_s represented the best overlap seen. The squeezed vacuum experienced quite large losses in propagation to the homodyne detector. The dominant factor here was the fact that the PPLN crystal was not antireflection coated at 1047 nm; the measured transmission for this wavelength was 76%. If it is assumed that the squeezed vacuum is generated in the center of the sample, then it only encounters a reflection loss at the exit face of the crystal. The magnitude of this depletion is $\sqrt{0.76} = 0.87$, which, combined with the losses in other optics in the squeezed beam path, led to an overall propagation factor of $\eta_p = 0.47$. Bringing together all of the individual loss mechanisms leads to an total quantum efficiency factor η of

$$\eta = \eta_d \eta_p \eta_s \eta_t = 0.16 \tag{5}$$

for detection of squeezed vacuum in PPLN. When measuring the noise level associated with a classical parametric gain G, the observed gain G_{obs} is given by [29,30]

$$G_{obs} = \eta G + 1 - \eta. \tag{6}$$

Using this expression, the measured amplification (3.9) and deamplification (0.46) factors in PPLN, and $\eta = 0.16$, it is expected that the noise power of the squeezed vacuum should reach 1.65 dB above and 0.7 dB below the SNL. These compare very well with the extrema of the squeezing curve in Fig. 5.

B. Model for observed squeezed vacuum noise

The discussion above attempted to find an agreement between the squeezing seen at one particular value of the LO phase, and the maximum classical gain of the PPLN amplifier. It is also possible to fit the squeezed vacuum data, over a range of LO phase values, to an equation which contains the phase dependence of the squeezing. As the phase of the LO is scanned, the noise at different phases, θ, is sampled so that [31,32]

$$P_\theta(\omega) = \eta G_\theta + 1 - \eta = \eta(e^{2r}\cos^2\theta + e^{-2r}\sin^2\theta) + 1 - \eta, \tag{7}$$

where ω is the rf detection frequency. Here the maximum classical gain ($G_+ = e^{2r}$) and minimum classical gain ($G_- = e^{-2r}$) of the amplifier are directly related to the squeezing parameter r. This results in a symmetric oscillation above and below the SNL which has $P_{SNL} = 1$. In an actual experiment, a rf amplifier is used to raise the squeezed signal well above the noise floor of the spectrum analyzer. The resulting noise power is the sum of this amplifier noise and the noise due to the amplified photocurrents:

$$P_\theta(\omega) = \{\eta(e^{2r}\cos^2\theta + e^{-2r}\sin^2\theta) + 1 - \eta\} \times P_{LO} G_{amp}(\omega) + P_{amp}. \tag{8}$$

P_{LO} is the LO noise power, $G_{amp}(\omega)$ is the frequency-dependent gain of the rf amplifier, and P_{amp} is the electronic background noise contributed by the rf amplifier. This last term can be measured by recording the noise power when the photodiodes are blocked but the amplifier is switched on, and is then subtracted from all subsequent readings. If squeezing is measured at a single detection frequency, as it was in this work, the frequency dependence of G_{amp} can be dropped from Eq. (8). Finally, because a spectrum analyzer usually measures the noise power in decibels, Eq. (8) is transformed to

$$P_\theta = 10\log_{10}\{\eta(e^{2r}\cos^2\theta + e^{-2r}\sin^2\theta) + 1 - \eta\} + P_{LO} G_{amp}. \tag{9}$$

Note that the term $P_{LO}G_{amp}$ is now just the measured SNL, in dB, after electronic background subtraction. This equation can then be used to estimate the value of detection efficiency and the initial level of squeezing from the measured squeezed vacuum data.

The squeezed vacuum of Fig. 5 was fitted to the model described by Eq. (9). However, because the amplification and deamplification responses of the PPLN parametric amplifier were not symmetrical (1/deamplification $\neq$ amplification), two curves were required to model the experimental data fully—one with $r = 0.68$ for amplification, and another having $r = 0.39$ for deamplification. Plots obtained from Eq. (9) with $\eta = 0.16$, and squeezing parameters of 0.68 and 0.39, are also shown in Fig. 5. Although the phase of the curves differs slightly from the experimental data points, the maximum and minimum noise powers of the model and the experiment do coincide. This model can be used to infer the squeezing level in PPLN for the case of perfect detection efficiency; with $\eta = 1$ in Eq. (9), the noise power reaches 6 dB above [$r = 0.68$ in Eq. (9)] and 3.3 dB below [$r = 0.39$ in Eq. (9)] the SNL. Therefore, we deduce 3.3 dB of noise reduction generated at 1047 nm in this PPLN sample.

One partial solution to the low value of η for detection of squeezing in PPLN would have been to antireflection coat the crystal at appropriate wavelengths. Taking this step would have increased the overall quantum efficiency by just 2%, resulting in about 0.85 dB of directly observable squeezing below the SNL. The problem of the temporal mismatch between the LO and squeezed fields would not have been so easily resolved. One approach would have been to use fiber-pulse compression to shorten the duration of the LO pulse, so that it was a better temporal match to the squeezed pulse [32]. This was considered but not implemented here, due to a lack of sufficient LO power to produce the correct amount of compression in practical lengths of fiber. Ap-

proaches taken by other workers include exploiting group-velocity dispersion at the frequency-doubling stage to lengthen the pump pulse, relative to the signal [33]. This longer pump pulse then generated a squeezed pulse which was slightly temporally broader than the LO used in the BHD; the entire LO pulse can then highlight the squeezing around the peak of the squeezed pulse. Finally, if the LO beam is passed through a device identical to the squeezer, for example a second parametric amplifier [34] or a dummy waveguide [33], the spatial overlap factor between the LO and squeezed beams can be improved [35].

VI. CONCLUSION

Experimental results were presented for degenerate parametric amplification, driven by an all-solid-state pulsed system, in two different nonlinear materials. Conventional birefringent phase matching was used with bulk $MgO:LiNbO_3$, which was found to suffer from photorefractive damage, but no such damage was observed with the quasi-phase-matched PPLN sample. It was found that, in both cases, the gain of the amplified and deamplified quadratures was asymmetric, and that the highest degree of asymmetry occurred in PPLN which also provided the largest amplification factor. This observation is consistent with gain-induced diffraction, which means that, for pumping with Gaussian beams, the portion of the signal beam that is closest to the propagation axis is amplified or deamplified more than light in the wings of the spatial profile. The same effect occurs in the temporal domain for pulsed parametric amplification. The higher the gain, the greater the spatial and temporal distortion of the signal field, and the greater the lack of agreement between amplification and inverse deamplification—the results differ more from the plane-wave case. The bulk PPN sample provided a parametric amplification of 3.9 (a deamplification of 0.46), and did not show any signs of photorefractive damage due to the high peak powers provided by the cw mode-locked system described here.

No further investigations were carried out using $MgO:LiNbO_3$ because of the complications introduced by the need to chop the mode-locked pulse train to reduce average pumping powers. Parametric fluorescence and quadrature-phase squeezing were recorded using bulk PPLN. The total average power of SPF generated in PPLN was estimated to be 2.4 nW; this was too low to allow us to measure the bandwidth of the fluorescence, and therefore the bandwidth of squeezing generated by the device. Using balanced homodyne detection, 0.5 dB of squeezing in the vacuum was observed directly. This agrees well with the total quantum efficiency, which was estimated by multiplying the individual components. The experimental phase-dependent squeezed vacuum data points were fitted to a simple model which contained the initial squeezing, and the homodyne detection efficiency, as free parameters. This theoretical model was used to infer 3.3 dB (or 53%) of initial squeezing generated in the bulk quasi-phase-matched PPLN sample. As is normal in these types of experiments, the parametric gain and squeezing data were recorded by averaging the photocurrents over the area of the optical beam which strikes the detector. Direct detection also has the effect of averaging the measurement over very many pulses, because the response time of the detectors used was slow compared to the duration of the laser pulses.

We have shown that it is possible to observe significant amounts of squeezing using bulk PPLN, despite the presence of some gain-induced diffraction. Central to our successful observation of squeezing was the cw mode-locked all-solid-state system that formed the starting point of the experiment. This system provided a reliable source of short pulses that could be used to drive the various nonlinear processes. The major advantage of diode pumping is the reduction in laser noise compared to a flashlamp-pumped source. When it comes to detection of squeezed light, it is important that all sources of extra noise in the experiment are eliminated. The laser output was checked rigorously to ensure that it provided shot-noise-limited performance. This meant that it was possible to observe 0.5 dB of noise reduction in the vacuum despite the low quantum efficiency of the detection scheme. The short duration of the mode-locked pulses implied very high peak powers for modest average powers, and this translated into high single-pass parametric gain and squeezing.

The various factors which may have affected the PPLN performance were discussed, as were possible steps which could be taken to remedy the low efficiency of detection for squeezing measurements. The detailed pulsed parametric gain and squeezing results presented in this paper clearly demonstrate the potential of bulk PPLN as a material capable of generating large quantum effects. Detailed studies, such as the one presented here, can help in the design of samples and experimental parameters which are optimized to produce large squeezing with high efficiency.

ACKNOWLEDGMENTS

The authors would like to thank Steve Barnett for many useful discussions, and the Optoelectronics Research Center in Southampton for the loan of the PPLN sample. This research was funded by the U. K. Engineering and Physical Sciences Research Council. E. M. D. is grateful for financial support provided by the European Comission.

[1] K. Bencheikh, E. Huntziger, and J.A. Levenson, J. Opt. Soc. Am. B **12**, 847 (1995).

[2] J.A. Armstrong, N. Bloembergen, J. Ducuing, and P.S. Pershan, Phys. Rev. **127**, 1918 (1962).

[3] V.S. Chickarmane and G.S. Agarwal, Opt. Lett. **23**, 1132 (1998).

[4] G.A. Magel, M.M. Fejer, and R.L. Byer, Appl. Phys. Lett. **56**, 108 (1989).

[5] L.E. Myers, R.C. Eckardt, M.M. Fejer, R.L. Byer, and W.R. Bosenberg, Opt. Lett. **21**, 591 (1996).

[6] W.R. Bosenberg, A. Drobshoff, J. Alexander, L.E. Myers, and R.L. Byer, Opt. Lett. **21**, 713 (1996).

[7] S.D. Butterworth, V. Pruneri, and D.C. Hanna, Opt. Lett. **21**, 713 (1996).
[8] G.D. Miller, R.G. Batchko, W.M. Tulloch, D.R. Weise, M.M. Fejer, and R.L. Byer, Opt. Lett. **22**, 1834 (1997).
[9] D.K. Serkland, M.M. Fejer, R.L. Byer, and Y. Yamamoto, Opt. Lett. **20**, 1649 (1995).
[10] M.E. Anderson, D.F. McAllister, M.G. Raymer, and M.C. Gupta, J. Opt. Soc. Am. B **14**, 3180 (1997).
[11] D.J. Lovering, J.A. Levenson, P. Vidakovic, J. Webjörn, and P.St.J. Russell, Opt. Lett. **21**, 1439 (1996).
[12] H.J. Eichler, P. Günter, and D.W. Pohl, *Laser-Induced Dynamic Gratings*, 1st ed., Springer Series in Optical Sciences Vol. 50 (Springer-Verlag, Berlin, 1986).
[13] L.E. Busse, L. Goldberg, M.R. Surette, and G. Mizell, J. Appl. Phys. **75**, 1102 (1993).
[14] J.R. Reitz, F.J. Milford, and R.W. Christy, *Foundations of Electromagnetic Theory*, 3rd ed. (Addison-Wesley, Reading, MA, 1979).
[15] D.H. Jundt, G.A. Magel, M.M. Fejer, and R.L. Byer, Appl. Phys. Lett. **59**, 2657 (1991).
[16] W.J. Kozlovsky, C.D. Nabors, and R.L. Byer, IEEE J. Quantum Electron. **24**, 913 (1988).
[17] G.D. Boyd and D.A. Kleinman, J. Appl. Phys. **39**, 3597 (1968).
[18] M.A. Persaud, J.M. Tolchard, and A.I. Ferguson, IEEE J. Quantum Electron. **26**, 1253 (1990).
[19] H.P. Yuen and V.W.S. Chan, Opt. Lett. **8**, 177 (1983).
[20] G.L Abbas, V.W.S. Chan, and T.K. Yee, Opt. Lett. **8**, 419 (1983).
[21] B.L. Schumaker, Opt. Lett. **9**, 189 (1984).
[22] A. La Porta and R.E. Slusher, Phys. Rev. A **44**, 2013 (1991).
[23] J.G. Rarity, P.R. Tapster, J.A. Levenson, J.C. Garreau, I. Abram, J. Mertz, T. Debuisschert, A. Heidmann, C. Fabre, and E. Giacobino, Appl. Phys. B: Photophys. Laser Chem. **55**, 250 (1992).
[24] C. Kim, R-D. Li, and P. Kumar, Opt. Lett. **19**, 132 (1994).
[25] E.M. Daly, A.S. Bell, E. Riis, and A.I. Ferguson, Phys. Rev. A **57**, 3127 (1998).
[26] H.P. Yuen and J.H. Shapiro, Opt. Lett. **4**, 334 (1979).
[27] D.A. Kleinman, Phys. Rev. **174**, 1027 (1968).
[28] R.M. Shelby and M. Rosenbluh, Appl. Phys. B: Photophys. Laser Chem. **55**, 226 (1992).
[29] P.D. Townsend and R. Loudon, Phys. Rev. A **45**, 458 (1992).
[30] H.-A. Bachor, *A Guide to Experiments in Quantum Optics*, 1st ed. (Wiley-VCH, Weinheim, 1998).
[31] T. Hirano and M. Matsuoka, Opt. Lett. **15**, 1153 (1990).
[32] T. Hirano and M. Matsuoka, Appl. Phys. B: Photophys. Laser Chem. **55**, 233 (1992).
[33] M.E. Anderson, M. Beck, and M.G. Raymer, Opt. Lett. **20**, 620 (1995).
[34] O. Aytür and P. Kumar, Opt. Lett. **17**, 529 (1992).
[35] M.V. Hobden and J. Warner, Phys. Lett. **22**, 243 (1966).